# Adaptive Color Matching via CNN and GRU Architectures with Optimization through Adaptive Cuckoo Algorithm

Yingdian Wang
College of Communication and Information Technology, Xi'an University of Science and Technology, Xi'an, 710600, China
E-mail: wangyingdian912@outlook.com

**Keywords:** convolutional neural network, deep learning, intelligent color matching, adaptive cuckoo algorithm, gated recurrent unit neural network

**Received:** July 4, 2025

*With the increasing influence of color on various fields, the current color matching technology that relies on manual color matching can no longer fulfill the color matching requirements of various fields. To meet the standardized and rational classification of colors and enhance the ability to match complex colors, an intelligent color matching technology based on convolutional neural network deep learning model is proposed. The research employs multi-layer convolutional networks to extract color space features, which are then combined with a gated recurrent unit neural network for modeling. The model captures color dependencies through gate updates and reset operations, followed by optimization via an adaptive cuckoo algorithm. Parameters are updated through Levy flight dynamics and dynamic elimination rules, enabling adaptive adjustments of step sizes and elimination probabilities with iteration counts. The model is ultimately applied to the DeepFashion dataset. During experiments, input data from the DeepFashion dataset were processed through feature layers using multidimensional tensors, ultimately generating RGB color schemes. The experimental results show that after 20 iterations of the model, the accuracy of the color matching method remains stable at around 93%, with a color difference range of 0.08-0.13 in warm tones and 0.03-0.06 in cool tones. In practical intelligent color matching, when the sample size of the color matching is increased to 10cm, the generation time of the color matching result stabilizes at around 2.8s, and the brand compatibility of the color matching result attains a 98% accuracy. The aforementioned results demonstrate that the intelligent color matching technology proposed in this research exhibits both high efficiency and accuracy. It effectively addresses the issues of sluggish color matching speeds and significant result errors prevalent in current color matching technologies, thereby enhancing the practicality of intelligent color matching solutions.*

*Povzetek: Razvita je metoda za inteligentno barvno ujemanje, ki združuje CNN za prostorske značilnosti, GRU za barvne zaporedne odvisnosti ter adaptivni kukavičji algoritem za optimizacijo parametrov. Model zazna nizke barvne razlike in doseže visoko ujemanje blagovne znamke.*

## 1 Introduction

Color matching (CM), as an element in information design, directly affects the aesthetic value of a work [1-2]. However, traditional CM methods rely on designer experience or rule-based algorithms based on theory, resulting in strong subjectivity, low efficiency, and difficulty in adapting to complex scenes. With the swift advancement of computer vision and deep learning (DL) technologies, intelligent color matching (ICM) has steadily emerged as a focal area of research [3]. However, early ICM technologies mainly focused on rule-based color blending algorithms and statistical-based color recommendation systems, which had high computational costs and were difficult to implement [4-5]. In summary, traditional CM techniques are unable to effectively meet CM requirements. Therefore, there is an urgent need for an ICM technology that can efficiently complete CM and meet design needs to a large extent. Convolutional Neural Network (CNN) has powerful feature extraction and pattern recognition capabilities, combined with emerging DL techniques, offering a novel approach to ICM. To meet the demand for CM technology, an innovative ICM technology based on CNNDL model is designed. The optimal CM parameters are selected by the optimization algorithm, and the generation efficiency and accuracy of the CM scheme are improved by CM samples and image data processing. Normalization and other operations are performed through CNN algorithm, and finally the optimal CM results are generated. The ICM in this research refers to a regression task that generates multi-color RGB palettes based on input images. Its objective is to minimize the color difference between generated results and actual color schemes while enhancing color harmony scores. The proposed methodology aims to provide theoretical support for ICM technologies in cultural fields, textile industries, and related scenarios. The research primarily addresses two key issues: (1) Algorithmic precision—Can the CNN-GRU hybrid model optimized with the adaptive cuckoo algorithm keep color difference values within industrial standard thresholds? (2) Generalization capability—Does the method achieve cross-tonal generalization across

warm and cool tone CM tasks?

## 2 Related works

In modern society, colors are everywhere, covering aspects such as daily life, healthcare, and transportation. Consequently, conducting research on ICM technology holds immense significance. Zhang et al. developed a task-based product CM design to deal with the lack of practical research on group collaboration. During the research process, the behavioral model of the designer was studied. The outcomes revealed that the research method could provide theoretical and practical basis [6]. Li et al. developed an Emocolor system to address the relationship between emotions and colors. The interactive genetic algorithm was optimized during the research process. The results indicated that the research method could effectively design emotional color schemes based on user emotions [7]. Zhou et al. studied the underwater image formation model and degradation theory to address the problem of difficulty in achieving visual expectations in images captured by cameras underwater. The existing underwater image dataset was reported during the research process. The results indicated that the research method could provide data support for future studies [8]. Wu et al. proposed a color coded intelligent digital loop mediated isothermal amplification method to address the issues of target specificity in most existing multiplex digital nucleic acid testing methods. An image analysis process was established during the research process. The outcomes indicated that the research approach had good effectiveness [9]. Haji et al. proposed an optimized artificial neural network model to address the issue of the impact of environmentally friendly coal dyes on dyed fabric samples. During the research process, different algorithms were used to optimize the neural network. The outcomes indicated that the research approach had high accuracy [10].

Numerous scholars around the world have undertaken comprehensive investigations and practical implementations related to CNNDL models. Ghosh et al. proposed an intelligent detection system for forest fires to address the serious threat they pose to the social environment. During the research process, a combination of CNNs and recurrent neural networks (RNNs) was used for feature extraction. The outcomes revealed that the research method had high classification accuracy [11]. Afshari Nia et al. proposed a DL model for predicting monthly rainfall for the problem of rainfall prediction. Combining DL models and artificial neural network models during the research process. The results indicated that the research method could simulate complex phenomena well [12]. Pekel Ozmen et al. proposed a system for predicting employee turnover in response to its impact on companies. A new hybrid extended convolutional decision tree model was developed during the research process. The results indicated that the research method could effectively predict employee turnover [13]. Zhang et al. proposed a coordinated mobile and residual transformer for precise segmentation of medical images. During the research process, a robot process automation module was added to the downsampling layer. The outcomes indicated that the research method could substantially enhance the accuracy of medical image segmentation [14]. Masud M et al. proposed different CNN models for the diagnosis and classification of breast cancer. A shallow custom CNN was proposed during the research process, and the outcomes indicated that the research approach had good classification capability [15]. The research on ICM is shown in Table 1.

Table 1: Comparison of ICM related research

| Author and Year | Dataset/Domain | Method | Evaluation indicators and performance |
|---|---|---|---|
| Zhang L et al. (2022) | Group collaboration design scenario | Task driven CM model | Provide theoretical basis without quantifying performance indicators |
| Haji A et al. (2023) | Cotton fabric dyeing sample | Optimize artificial neural networks | High accuracy, without indicating cross material generalizatio n ability |
| Ghosh R et al. (2022) | Forest fire images | CNN+R NN | High classification accuracy, but not tested in complex lighting scenarios |
| Pekel Ozmen et al. (2022) | Enterprise employee data | Mixed Convoluti onal Decision Tree | Loss prediction is effective, but the accuracy of small sample scenarios decreases |

As shown in Table 1, existing ICM methods suffer from issues such as weak scene adaptability, poor cross-tonal generalization capabilities, and an imbalance between efficiency and accuracy. Employing CNN for spatial feature extraction and integrating GRU to capture temporal dependencies in color patterns can enhance cross-scene adaptability. The dynamic-step cuckoo algorithm further enables differentiated adjustments of chromaticity thresholds in warm/cold tone scenarios. Building on these advancements, this study proposes an ICM technology based on CNN convolutional DL models. This approach aims to meet design requirements in smart CM systems while improving both precision and practical applicability.

# 3 ICM technology methods

## 3.1 Construction of ICM system

Color is extremely important in daily life, and currently the commonly-used CM methods are mainly manual CM, which is frequently impacted by elements like the mood and experience of the colorist [16]. ICM technology can effectively avoid the influence of external factors on CM results. The research constructs a computer ICM model using neural network algorithms. The ICM system framework is presented in Figure 1.

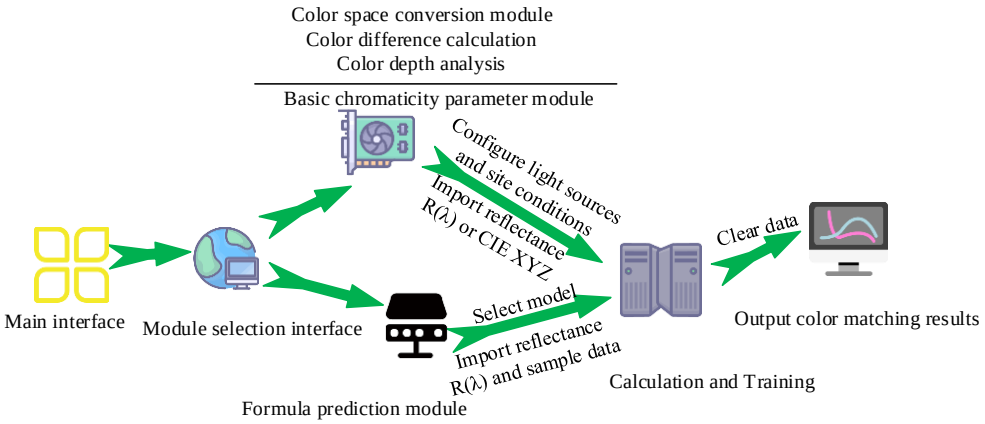


Figure 1: Framework of computer ICM system

As illustrated in Figure 1, the computerized ICM system takes the main interface as the entrance, and users can select functional modules according to their needs. The basic chromaticity parameter module includes color space conversion module, color difference calculation, color depth analysis and other functions. It supports importing reflectance R (λ) or standard chromaticity system data formulated by the International Commission on Illumination, and configuring light sources and on-site conditions for calculation. The color prediction module imports the reflectance R (λ) and the sample data of the desired color chart, selects the prediction model for training, and finally outputs the CM results. Each module is equipped with a data clearing and export module, supporting user management operations. The nonlinear least squares optimization algorithm can be used for weight and bias adjustment in backpropagation neural networks, and its iterative formula is presented in equation (1).

$$\begin{cases} J(w)=\frac{1}{2}\sum_{i=1}^{N}(y_i-f(x_i,w))^2 \\ \Delta w=-[J^TJ+\mu diag(J^TJ)]^{-1}J^Te \end{cases} \quad (1)$$

In equation (1), $J(w)$ is the error function, $w$ is the parameter vector of the model, $N$ denotes the overall quantity of training samples, $y_i$ is the actual output of the $i$ th sample, and $f(x_i,w)$ is the forecasted output for the input. $\Delta w$ is the update quantity of parameter $w$, $J$ is the Jacobian matrix, $J^T$ is the transpose of the Jacobian matrix, $\mu$ is the damping parameter, $diag()$ is the diagonal matrix, and $e$ is the error vector. Inverse normalization is performed on the output results to obtain the same CM data as the original, as shown in equation (2).

$$y_{raw}=y_{norm}\times(y_{max}-y_{min})+y_{min} \quad (2)$$

In equation (2), $y_{raw}$ is the output value after inverse normalization, $y_{norm}$ is the output value after normalization, $y_{\max}$ and $y_{\min}$ is the max and min values of the feature in the original data. For the output results, Bayesian algorithm is firstly chosen for posterior probability calculation, and the calculation formula is presented in equation (3).

$$P(A|B)=P(B|A)*P(A)/P(B) \quad (3)$$

In equation (3), $P(A|B)$ is the posterior probability of the event occurring, $B$ is the initial probability of the event occurring, and $A$ is the total probability of the event occurring. A decision function is constructed based on the obtained results, and judgments are made on the results. The function formula is presented in equation (4).

$$f(x)=sign(m\cdot\Phi(x)-\rho) \quad (4)$$

In equation (4), $f(x)$ is the decision function, $sign(\cdot)$ is the sign function, $m$ is the weight vector, $\Phi(x)$ is the mapping function, and $\rho$ is the bias of the decision boundary. The ICM technology based on machine learning is also a traditional and common method for ICM, and its basic functional modules are presented in Figure 2.

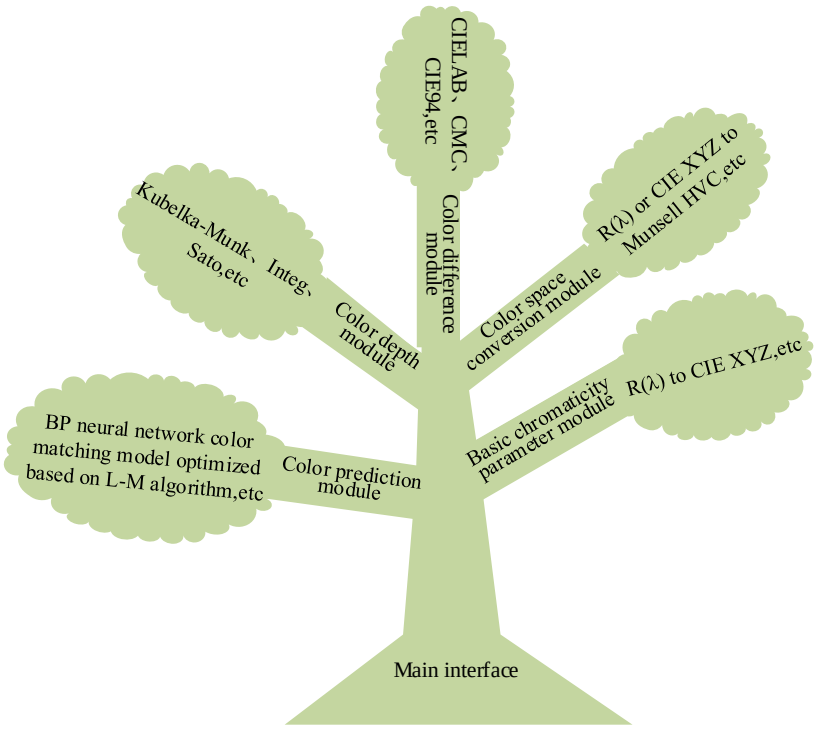


Figure 2: Function of machine learning CM system

As shown in Figure 2, after entering the ICM system based on machine learning from the main interface entrance, it will implement color processing and prediction functions through five core modules. The basic chromaticity parameter module handles the fundamental conversion of color physical properties. It facilitates the mutual calculation between reflectance R(λ) and data from international standard chromaticity spaces, such as those defined by the International Commission on Illumination's standard chromaticity system. The color space conversion module performs multidimensional mappings between various color models. It supports conversions from R(λ) or data from the standard chromaticity systems established by the International Commission on Illumination to the Munsell color classification and description systems, as well as other relevant standards. The color difference module integrates algorithms such as color space, quantifies color differences, and adapts to the accuracy requirements of various industries. The color depth module calculates depth dimensions such as color saturation through Kubelka Munk, Integ, Sato and other models, providing corresponding parameter support for color scheme adjustment. The color prediction module, combined with models such as the Back Propagation neural network CM model optimized based on the Levenberg Marquardt algorithm, presents a technical process visualization structure of information. AregressionalLayer algorithm is added at the end of the ICM system model to verify its reliability, and its calculation is presented in equation (5).

$$loss = \frac{1}{\mathrm{n}} \sum_{i=1}^{n} \left( y_i - y_i \right)^2 \quad (5)$$

In equation (5), $loss$ is the mean square error loss value of the model, $n$ is the number of samples, $y_i$ and $y_i$ is the actual and forecasted values of the $i$ th sample. For the selection of the activation function (AF) for the model activation layer, the LeakyRelu function is used in the study, and its calculation is presented in equation (6).

$$g(x) = \begin{cases} x, x \geq 0 \\ \alpha x, x < 0 \end{cases} \quad (6)$$

In equation (6), $g\left(x\right)$ is the output value of the AF, $x$ is the input value of the neuron, and $\alpha$ is the negative slope coefficient. Another common ICM technology is based on fully connected neural network DL models, which have better accuracy compared to machine learning based ICM technology. The flowchart is presented in Figure 3.

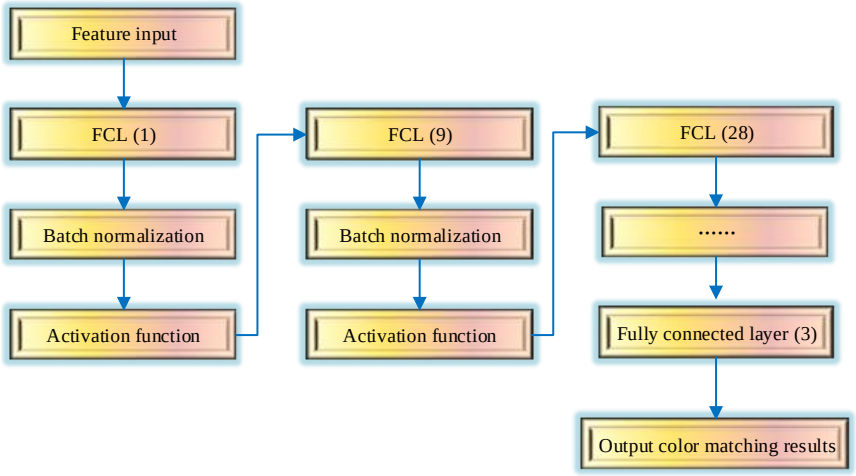


Figure 3: A fully connected neural network DL model

As illustrated in Figure 3, the ICM technology based on fully connected neural network DL model first inputs the features of the CM map into the system, then enters the fully connected layer (FCL) for batch normalization, and inputs the processed CM data into the AF for activation. Following this, the data feeds into another FCL, where batch normalization and activation processes are carried out repeatedly. This iterative procedure continues until the user's specified criteria are fulfilled, at which point the CM results are generated. In context, it can be concluded that the traditional ICM system shown in Figure 1 to Figure 3 has limitations in complex scene adaptability, computing efficiency and CM accuracy. The CNN convolutional DL model proposed in subsequent research is mainly aimed at breaking through these bottlenecks.

## 3.2 ICM method based on CNNDL model

Although ICM technology based on traditional methods has better efficiency compared to manual CM methods, environmental factors produce a more profound effect on the outcomes and still have significant errors in accuracy. CNNDL algorithms can handle complex nonlinear relationships, parallel computing, and real-time applications, with good data processing capabilities and reliability [17]. The model structure diagram is presented in Figure 4.

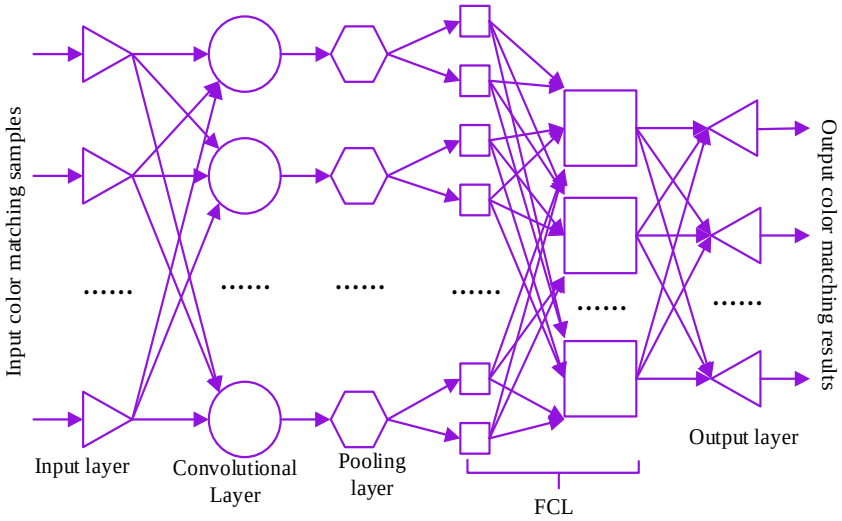


Figure 4: CNNDL model structure

As illustrated in Figure 4, the CNNDL model is mainly divided into five layers. The CM samples first enter the input layer, which performs simple processing on the CM samples before inputting them into different convolutional layers. After repeated normalization and activation processing through convolutional layers, the CM sample data is input to the corresponding specific pooling layer, and then input to the adjacent FCL. Finally, different color samples are output from different standard output layers to achieve ICM of the color samples. Specifically, the input layer of CNN receives preprocessed RGB images. The feature extraction section comprises three convolutional blocks: each block consists of a convolutional layer (kernel size $3\times3$, stride 1, padding 'same'), a batch normalization layer, and a LeakyReLU activation layer ( $\alpha$ =0.1). The number of filters in these blocks is 32,64, and 128 respectively. Each convolutional block is followed by a $2\times2$ max pooling layer (stride 2). The extracted feature maps are

arranged in spatial sequence and fed into the GRU model. When the model receives image samples that require CM, the convolution kernel performs feature extraction on them, and the extraction formula is presented in equation (7).

$$\alpha_{i,j}= f\left(\sum_{m=0}^{k-1}\sum_{n=0}^{k-1}\omega_{m,n}x_{i+m,j+n}+\omega_b\right) (7)$$

In equation (7), $\alpha_{i,j}$ is the local features of the input image extracted by the convolution kernel, $f()$ is the AF, $\omega_{m,n}$ is the weight parameters of the $m$ th row and $n$ th column in the convolution kernel, $x_{i+m,j+n}$ is the feature values of the $(i+m)$ th row and $(j+n)$ th column in the input image, $\omega_b$ is the bias term, and $k$ is the size of the convolution kernel. To further explore the feature information of CM image samples, a feature extraction model is constructed, and the model calculation formula is presented in equation (8).

$$\alpha_{i,j}= f\left(\sum_{d=0}^{D-1}\sum_{m=0}^{k-1}\sum_{n=0}^{k-1}\omega_{m,n}x_{d,i+m,j+n}+\omega_b\right) (8)$$

In equation (8), $D$ is the number of channels in the input data, $x_{d,i+m,j+n}$ is the feature values of the $(i+m)$ th row and $(j+n)$ th column of the $d$ th channel in the input image, where $\omega_{m,n}$ does not vary with channel $d$. Therefore, the convolutional layer function of the CNNDL model is presented in Figure 5.

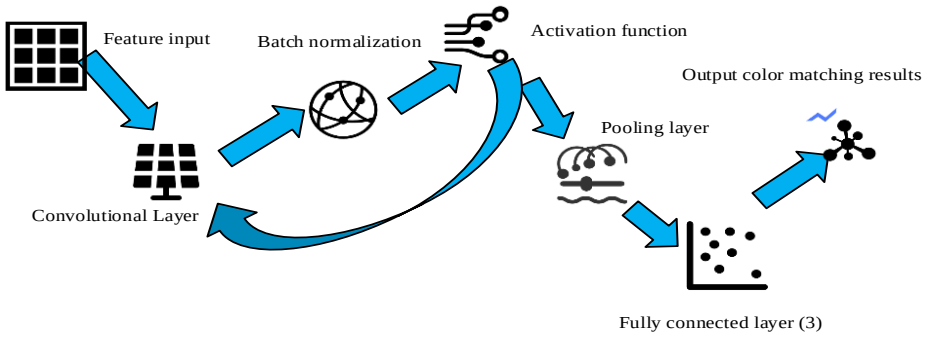


Figure 5: CNNDL model with convolutional layer functions

As shown in Figure 5, the convolutional layer of the CNNDL model mainly normalizes the feature vectors extracted from CM samples in batches, and inputs the normalized data into the AF for calculation, which is repeatedly executed twice. This process forms the essence of circular convolution layer optimization. It deepens feature extraction by conducting two iterations of convolution-normalization-activation operations. This approach differs from the time cycle mechanism employed by GRU in the subsequent stage. The data processed by the convolutional layer is then input into the pooling layer and FCL until the final regression output. The study uses the cuckoo algorithm to solve the updated mathematical expression in the ICM model framework of CNNDL. The algorithm formula is presented in equation (9).

$$\begin{cases} x_{j+1,i}=x_{j,i}+\alpha s\left(x_{j,i}-x_{j,best}\right) \\ s \sim \dfrac{\Phi u}{|v|^{\frac{1}{\beta}}} \end{cases} (9)$$

In equation (9), $x_{j+1,i}$ is the new position of the $i$ th nest in the $j+1$ th generation population, $x_{j,i}$ is the current position, $\alpha$ is the step size scaling factor, $s$ is the Levy flight step size, $x_{j,best}$ is the optimal nest in the $j$ th generation population, $\beta$ is the parameters of the Levy distribution, and $\Phi$ is the normalization constant. The expression for $\Phi$ is presented in equation (10).

$$\Phi=\left[\frac{\Gamma(1+\beta)\sin\left(\pi\frac{\beta}{2}\right)}{\Gamma\left\{\left[1+\frac{\beta}{2}\right]\beta 2^{\frac{\beta-1}{2}}\right\}}\right] (10)$$

In equation (10), $\Gamma$ is the Gamma function. During the update process, image data that requires CM will be randomly eliminated, and the expression of the elimination rule is presented in equation (11).

$$x_{j+1,i}=x_{j,i}+heaviside[rand(1),P_a]\left(x_{j,m}-x_{j,best}\right) (11)$$

In equation (11), $heaviside()$ is the Heaviside function, $rand(1)$ is a random number uniformly distributed within $[0,1]$, $P_a$ is the elimination probability, and

$x_{j,m}$ is another nest randomly selected from the $j$ th generation population $(m \neq i)$. However, there is uncertainty in both the Levy flight and elimination rules. Therefore, to enhance the global search ability for CM image data, the adaptive cuckoo algorithm is adopted in the study, and its expression is presented in equation (12).

$$\begin{cases} \alpha = \alpha_{min} + \left(\alpha_{max} - \alpha_{min}\right)\left(\dfrac{N_{UM} - j}{N_{UM}}\right)^{m_1} \\ P_a = P_{a,min} + \left(P_{a,max} - P_{a,min}\right)\left(\dfrac{N_{UM} - j}{N_{UM}}\right)^{m_2} \end{cases} \quad (12)$$

In equation (12), $\alpha_{\min}$ and $\alpha_{\max}$ are the min and max values of the step size scaling factor, $N_{UM}$ is the max iteration count, and $j$ is the current iteration count, $\left(j = 1, 2, \ldots, N_{UM}\right) \cdot m_1$ and $m_2$ are the adjustment factors, and $P_{a,\min}$ and $P_{a,\max}$ are the min and max values of the elimination probability. At the end of the CNNDL model, the average absolute error and absolute coefficient algorithms are selected for evaluation, where the expression of the average absolute error is presented in equation (13).

$$MAE = \frac{1}{n}\sum_{i=1}^{n}\left|y_{pred_i} - y_i\right| \quad (13)$$

In equation (13), $MAE$ is the average absolute error, $y_{pred_i}$ is the predicted value of the model for the $i$ th sample, and $y_i$ is the true value of the $i$ th sample. The expression for the absolute coefficient is presented in equation (14).

$$R^2 = 1 - \frac{\sum_{i=1}^{n}\left(y_{pred_i} - y_i\right)^2}{\sum_{i=1}^{n}\left(y_{mean} - y_i\right)^2} \quad (14)$$

In equation (14), $R^2$ is the coefficient of determination and $y_{mean}$ is the mean of the true values of all samples. In conclusion, the study employs a composite loss function structure. This structure utilizes chromaticity loss to gauge the absolute difference between predicted and real color values, while also incorporating style consistency loss to ensure the color scheme aligns well with brand and cultural characteristics. The final research aims to develop an ICM model capable of effectively capturing long-term dependencies in color sequences, thereby achieving precise CM over extended periods. The gating recurrent unit architecture demonstrates superior computational efficiency compared to LSTM, while maintaining effective detection of short-term color sequence dependencies. Consequently, this study integrates a gating recurrent unit neural network model, as expressed in Equation (15).

$$\begin{cases} z_t = sigmiod\left(W_z\left[h_{t-1}, x_t\right] + b_z\right) \\ r_t = sigmiod\left(W_r\left[h_{t-1}, x_t\right] + b_r\right) \\ h_t' = tanh\left(Wh\left[r_t h_{t-1}, x_t\right] + b_h\right) \\ h_t = \left(1 - z_t\right)h_{t-1} + z_t h_t' \\ y_t = W_y h_t + b_y \end{cases} \quad (15)$$

In equation (15), $z_t$ is the update gate (UG), $r_t$ is the reset gate (RG), $h_t'$ is the candidate state (CS), $h_t$ is the current state, $h_{t-1}$ is the hidden state from the previous time, $x_t$ is the color map features extracted by the CNNDL model, and $y_t$ is the output map features. $W_z, W_r, W_h, W_y$ are the weight matrices for the UG, RG, CS, and output layer. $b_z, b_r, b_h, b_y$ correspond to the bias terms of each layer. The input sequence length is fixed to 4 steps, which represents the correlation span of each color feature block extracted from CNN in the time dimension. In summary, the basic process of researching an ICM model based on CNNDL model is presented in Figure 6.

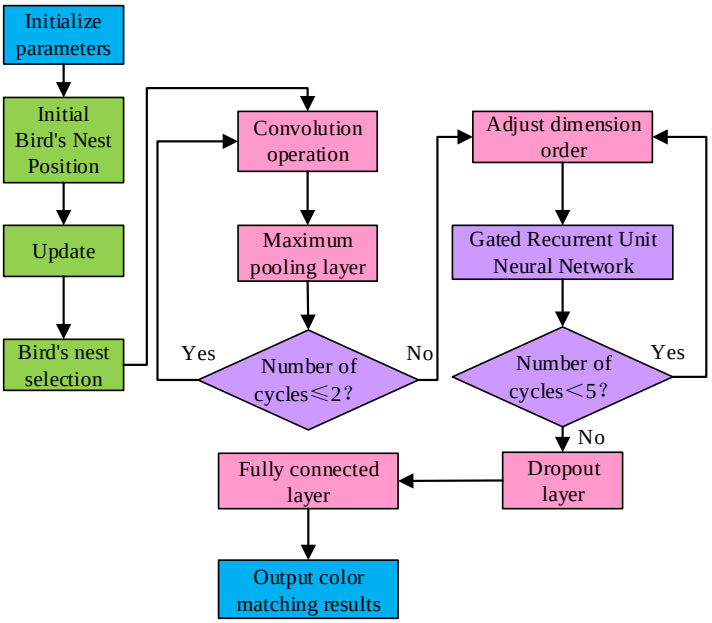


Figure 6: Flow chart of CNNDL model

As illustrated in Figure 6, the ICM technology based on CNNDL model first inputs the initialized CM samples into the initial nest position of the adaptive cuckoo algorithm, and then updates and selects the optimal CM parameter combination according to the Levy flying nest and elimination rule. Subsequently, the results feed into a CNN to undergo convolution operations and then integrate with a gated RNN for looping processing. When the CM sample cycles through the convolutional layer more than twice, the system can adjust the dimension order accordingly. The dimension adjustment sequence refers to reorganizing the three-dimensional feature tensor output by CNN into a two-dimensional sequence to meet the processing requirements of GRU for time-series data. The iteration termination condition for convolution layers is defined as occurring when the iteration count surpasses two. This ensures that, after two convolutions, the feature extraction process advances to the dimension transformation stage, thereby guaranteeing thorough feature extraction. When the adjusted color samples are cycled more than four times in the gated RNN, they are input into the Dropout layer and FCL for final processing, completing the regression output and achieving ICM of the color samples. The sizes of the convolution kernels in the model are 3*3 for the first layer and 5*5 for the deep layer. The network consists of 4 convolution layers and 2 full connection layers. A Dropout layer is set in front of the full connection layer with a dropout rate of 0.3. Two GRU layers are stacked, and the hidden layer dimension is aligned with the output of CNN.

# 4 Verification of CM technology based on CNNDL model

## 4.1 Performance testing of ICM technology

To verify the performance of ICM technology based on CNN DL model, a simulation model was constructed for testing. The experiment adopted DeepFashion data set, which contains 8,000 clothing images and labels. All input images were uniformly scaled to 224*224 pixels, and the RGB values of pixels were normalized to [0,1] range. The testing environment and specific configuration are presented in Table 2.

Table 2: Test Environment and specific configuration

| Testing environment | Specific configuration |
|---|---|
| Color measurement equipment | Spectrophotometers (the CS-580 and TS7 series) |
| Computing equip-ment | High-performance processors (STM32 F429/F439) and ex-tended storage (BBA-IS364) |
| Interactive device | VR helmet (3Glasses S2), Data Glove (Cyberglove II) |
| Operating system | Support multiple platforms (Windows/Linux) |
| CM toolchain | PeColor/MatchColor CM soft-ware |
| Database | MySQL or MongoDB stores color samples and formula data |

Performance testing of the CM model was conducted in a simulated environment configured as shown in Table 2. The interaction process between hardware/software and algorithms in this environment was as follows: Color measurement devices collected reflectance data from target samples, which were then input into the system's chromaticity parameter module to complete color space conversion and chromaticity calculation. Interactive devices displayed matching schemes in real-time while receiving user feedback. The database stored preprocessed results from the DeepFashion dataset for instant loading during model training. The optimizer adopted Adam, the initial learning rate was set to 0.001, and the decay rate was 0.5 for every 10 epochs. The training batch was fixed at 64, the test batch was 32, and the maximum iteration was 100 times. To improve the

generalization ability of the model, the study used 10-fold cross-validation to train and test the model for many times. All experimental results were based on the mean value of 5 independent repeated experiments, and the 95% confidence interval was calculated. The research method was compared with the harmony algorithm and neural network algorithm. The core of the harmony algorithm was to realize parameter search through normalized color harmony and Levenberg-Marquardt optimization of back propagation neural network. The neural network algorithm is an end-to-end CM prediction with basic DL capability through multi-layer full connection structure. The study compared the accuracy changes of each method model under different training iterations, and the outcomes are presented in Figure 7.

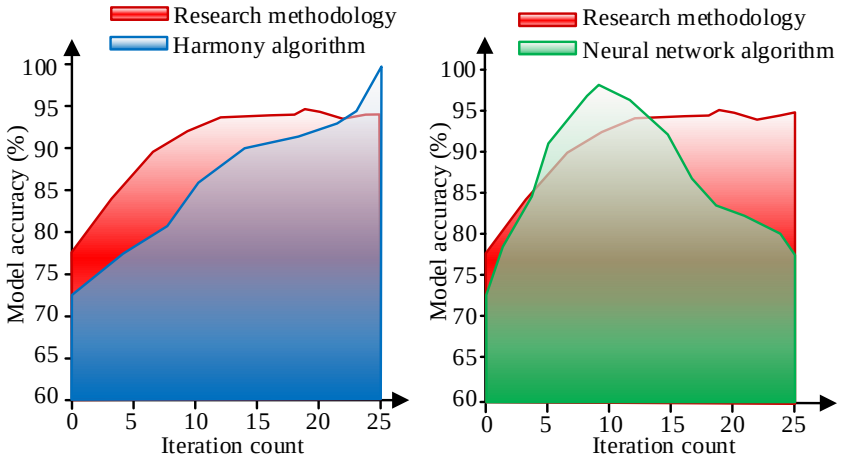


(a) Research methodology VS Harmony algorithm

(b) Research methodology VS Neural network algorithm

Figure 7: Comparison of model accuracy under different iterations

As shown in Figure 7, the model accuracy of the research method gradually increased with the number of iterations. However, after reaching 20 iterations, the model accuracy gradually stabilized at around 93%, which largely met the fitting standards. As shown in Figure 7 (a), the model accuracy of the harmonic algorithm continues to increase with different iterations, and there was an abnormal increase in the accuracy at the 23rd iteration. As shown in Figure 7 (b), the model accuracy of the neural network algorithm increased rapidly as the number of iterations increased, but after eight iterations, it started to go down. The results of paired *t*-test showed that the final test accuracy of the research method (93.2% ±1.5%,95% CI [92.8%,93.6%]) was significantly higher than that of the harmonic algorithm (85.7%±3.2%,95% CI [84.9%,86.5%], $t(799)=45.1$, $p<0.001$) and the neural network algorithm (78.3% ± 4.8%,95% CI [77.5%,79.1%], $t(799)=62.8$, $p<0.001$). Overall, the research method had better environmental adaptability compared to the comparative method. The research method was compared with the comparative method in terms of color difference values of different tones and color harmony scores of different methods, and the outcomes are presented in Figure 8.

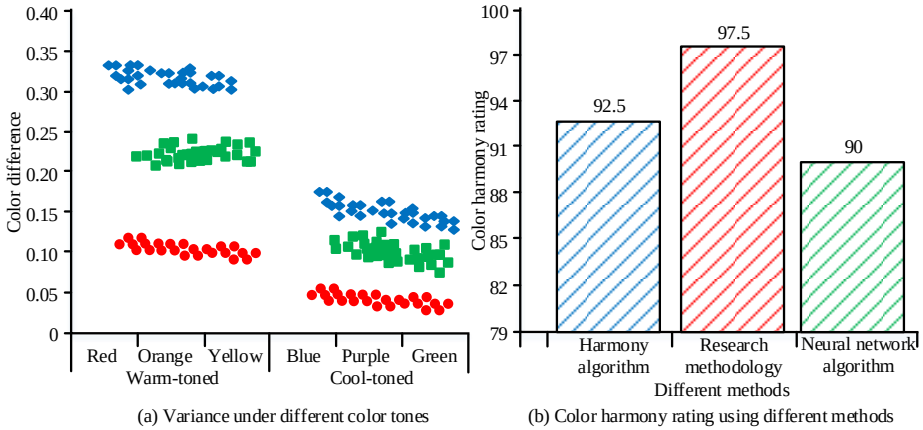


(a) Variance under different color tones

(b) Color harmony rating using different methods

Figure 8: Color difference values and color harmony scores for different color tones

As shown in Figure 8 (a), in the color difference value distribution of different methods under different tones, the harmony algorithm concentrated in the range of 0.3-0.35 for warm tones and 0.15-0.20 for cool tones. The

neural network algorithm had a color difference value in the range of 0.20-0.25 for warm tones and 0.08-0.15 for cool tones. The color difference range of the research method was 0.08-0.13 for warm tones and 0.03-0.06 for cool tones, and the distribution of each color in the two tones was uniform, while the two comparison methods were more focused on one color. Therefore, the prediction error of the research method was relatively small under different color tones. As shown in Figure 8 (b), statistical analysis showed that the color harmony score of the research method (97.5±1.2,95% CI [97.3,97.7]) was significantly higher than that of the harmonic algorithm (92.5±2.8,95% CI [92.1,92.9], $p$<0.001) and the neural network algorithm (90.0±3.5,95% CI [89.5,90.5], $p$<0.001).

## 4.2 Actual application effect of ICM technology

By verifying the capability of the ICM technology based on the CNN DL model, the practical application worth of the research approach was further substantiated. The research used the industrial tool chain to build a simulated CM platform for cultural and creative and clothing design. Pantone Textile Color System data set was adopted, which contained more than 2,300 textile industry standard color cards, covering the color reflectance data of cotton, silk, chemical fiber and other materials, as well as the corresponding chromatic coordinates of the International Lighting Commission. Comparing the research methods with the harmony algorithm and neural network algorithm, the time required for the three methods under different color quantities and graphic sizes is presented in Figure 9.

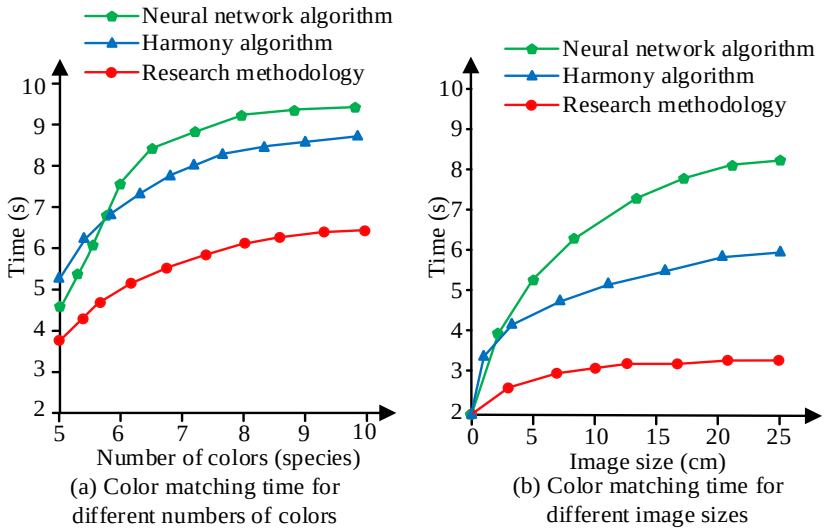


Figure 9: Generation time of different numbers of colors and image sizes

As shown in Figure 9 (a), as the number of colors in the CM sample increased, the generation time of the color scheme gradually rose for the three methods, and the increasing trend gradually slowed down. When the CM samples of the harmony algorithm increased from five colors to ten colors, the CM scheme generation time increased by 3 seconds, and the CM scheme generation time of the neural network algorithm increased by 4.5 seconds. For the research method, when the CM samples increased from five colors to ten colors, the CM scheme generation time rose from 3.9 seconds to 6.1 seconds, with a time increase of 2.2 seconds. As shown in Figure 9 (b), as the size of the CM sample image increased, the CM scheme generation time of the three methods increased logarithmically. The color scheme generation time of the harmony algorithm finally stabilized at around 5.5 seconds, while the color scheme generation time of the neural network algorithm gradually stabilized at around 8.2 seconds. The generation time of the color scheme of the research method changed little with the size of the image. When the image size increased to 10cm, it gradually stabilized at 2.8±0.2s (95% CI). Overall, research methods had better efficiency compared to comparative methods. In the realms of cultural creativity and branding, Figure 10 presents the comparative outcomes of cultural creativity CM results generated by various methods, evaluated based on criteria such as accuracy and creativity. Additionally, it showcases the results pertaining to brand CM, assessed in terms of efficiency and brand-fit.

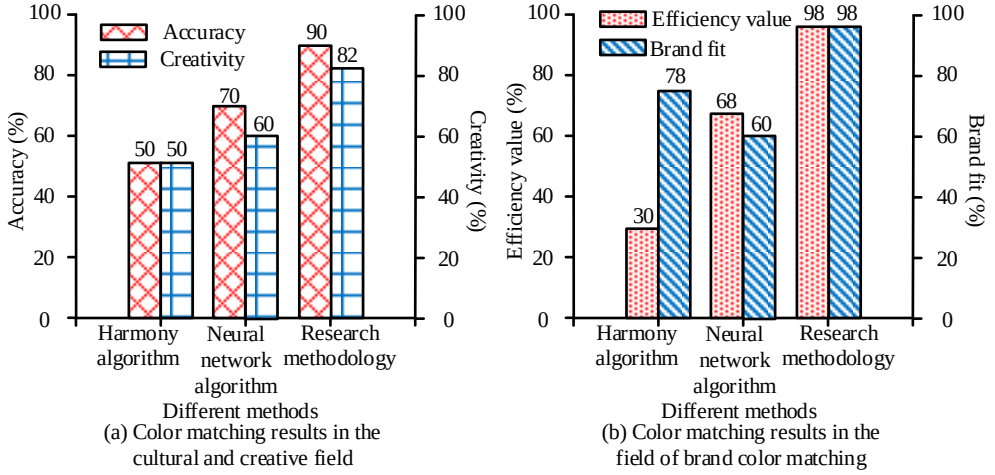


(a) Color matching results in the cultural and creative field

(b) Color matching results in the field of brand color matching

Figure 10: Comparison of CM results in two fields

As shown in Figure 10 (a), in the field of cultural and creative, the proportion of accuracy and creativity of CM results generated by research method was 90%±1.2% and 82%±2% respectively, which was far greater than that of harmony algorithm and neural network algorithm. As shown in Figure 10 (b), in the brand CM results, the efficiency value and brand fit of the research method both reached 98%±0.5%, which was far greater than that generated by the harmony algorithm and the neural network algorithm. Overall, the research method had better scene adaptability compared to the comparative method. The CM results of different methods were compared with the standard deviation of different sample sizes and the percentage of standard deviation under various test times, as presented in Figure 11.

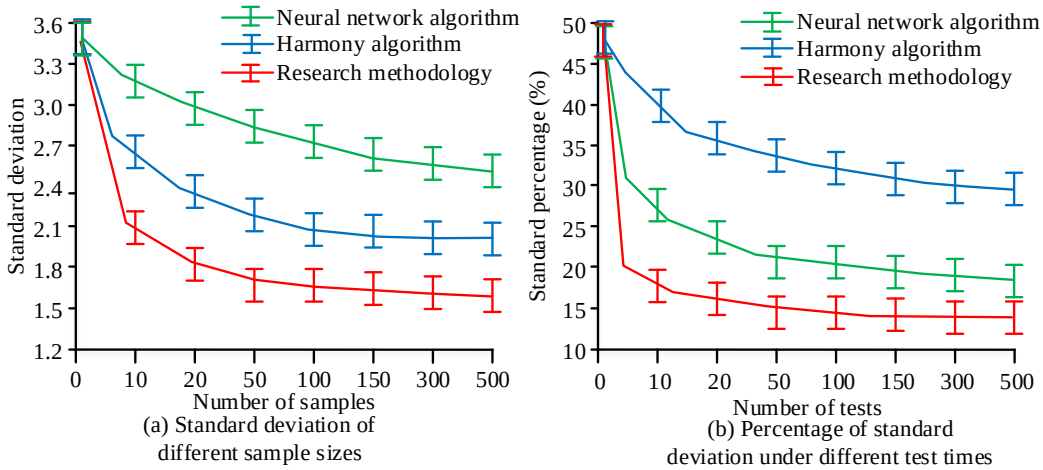


(a) Standard deviation of different sample sizes

(b) Percentage of standard deviation under different test times

Figure 11: Deviation of different sample sizes and various test times

As presented in Figure 11, the three methods exhibited a decreasing trend in the percentage of standard deviation for different sample sizes and test times. As presented in Figure 11 (a), the standard deviation of the CM results of the neural network algorithm gradually decreased as the sample size increased, and the decreasing trend became less pronounced. When the sample size was 500, the standard deviation was 2.8. The standard deviation of the CM results of the harmony algorithm and the research method gradually stabilized when the sample size increased to 150, with the harmony algorithm having a standard deviation of 2.3 and the research method having a standard deviation of 1.7. As shown in Figure 11 (b), the percentage of standard deviation of the CM results of the harmony algorithm and the neural network algorithm gradually decreased as the number of testing times increased, but the decreasing trend gradually slowed down. When the testing times were 500, the standard deviation percentage of the harmony algorithm was 35%, and the standard deviation percentage of the neural network algorithm was 23%, and the standard deviation percentages of the two methods still showed a downward trend. The percentage of standard deviation of the research method tended to stabilize when the number of tests was 150. When the number of tests was in the range of 150-500, the percentage of standard deviation of the CM results of the research method remained stable at around 15%. Overall, the research method had higher algorithmic accuracy. In summary, the intelligent CM technology based on the CNN DL model proposed by the research had good efficiency, scene adaptability, and algorithm accuracy.

### 4.3 Optimization algorithm comparison experiment

To evaluate the optimization performance of the Adaptive Cuckoo Search (ACS) algorithm, this study conducted ablation experiments comparing it with the Standard Cuckoo Search (SCS), Particle Swarm Optimization (PSO), Genetic Algorithm (GA), and no optimization method. All tests were performed on identical datasets and hardware configurations, with evaluation metrics including model accuracy, color difference (ΔE), CM generation time, and standard deviation. The experimental results are presented in Table 3.

Table 3: Optimization algorithm performance comparison

| Algorithm | Number of iterations (up to 93% accuracy) | Warm tones ΔE | Cool tone ΔE | Generation time (s) | Standard deviation (sample size =150) |
|---|---|---|---|---|---|
| ACS | 20 | 0.10±0.03 | 0.05±0.01 | 2.8 | 1.7 |
| SCS | 35 | 0.18±0.05 | 0.09±0.03 | 4.2 | 2.5 |
| PSO | 28 | 0.15±0.04 | 0.07±0.02 | 3.5 | 2.1 |
| GA | 42 | 0.21±0.06 | 0.11±0.03 | 5.1 | 3.0 |
| No optimization | Not convergent | 025±0.08 | 0.15±0.04 | 1.9 | 3.8 |

As shown in Table 3, ACS maintained an accuracy rate of 93% after 20 iterations, demonstrating the fastest convergence speed. Its chromaticity values and standard deviations were significantly lower than those of other algorithms. Notably, ACS's computation time was only slightly longer than the unoptimized approach, indicating that optimization calculations incur additional overhead. Experimental results showed that the ACS-optimized model outperformed both traditional optimization methods and unoptimized approaches in terms of efficiency and precision.

### 4.4 Practical application cases

For fashion design, designers applying the research methodology first inputted garment sketches or fabric images. The system then extracted color space features through CNN, captured color sequence dependencies via GRU, optimized color parameters using adaptive cuckoo algorithm, and ultimately outputted RGB color schemes. In digital media applications, the methodology began with scene screenshots or keyword inputs. It integrated emotional semantic features and modeled color-emotion associations through gating recurrent units to generate harmonious color schemes. For manufacturing, the process started with product reflectance or chromaticity data. The chromaticity module converted these into color spaces, while the color prediction module calculated saturation using the Kubelka-Munk model. The final formula data were stored in MongoDB database.

## 5 Discussion

### 5.1 Comparative analysis of experimental results

The ICM technology proposed by the research demonstrated significantly superior performance metrics compared to conventional contrast-based methods. The accuracy rate of this approach stabilized at 93%, substantially outperforming both harmonic algorithms and neural network algorithms. Notably, it outperformed harmonic algorithms in both warm and cool tone color differences, while outperforming neural network algorithms in warm tone color differences. When processing samples ≥10cm, the matching generation time stabilized at 2.8 seconds – notably shorter than harmonic algorithm's 5.5 seconds and neural network algorithm's 8.2 seconds. This breakthrough demonstrated the method's capability to transcend traditional limitations of manual rule-based approaches or superficial statistical models, achieving deep modeling of complex color relationships.

### 5.2 Core mechanism of performance advantage

The key to the research's leading method performance lies in technological innovation. The study adopted a spatiotemporal feature fusion mechanism, where the GRU gated recurrent unit captured long-term dependencies in color sequences to enhance temporal chromatic coherence. By aligning CNN-extracted local color features with GRU's temporal encoding, it achieved lossless spatiotemporal feature integration. The adaptive cuckoo algorithm dynamically adjusted Levy flight step size and elimination probability, preventing traditional optimization algorithms from getting trapped in local optima. During iteration, the step size scaling factor underwent algebraic self-adaptive decay, balancing global exploration with fine-grained local search.

### 5.3 Unexpected discovery and performance tradeoff

Experimental results demonstrated that the color difference of cool tones was significantly lower than that of warm tones, which might be attributed to the more concentrated distribution of cool tones in the LAB color space. Future research could focus on designing differentiated feature extraction modules based on hue characteristics. Although the proposed method improved accuracy through the introduction of GRU and adaptive optimization, the increased number of model parameters resulted in higher computational costs for small sample scenarios. However, when sample complexity was enhanced, the parallel computing advantage became evident, stabilizing computation time at 2.8 seconds, thereby validating the method's applicability for large-scale tasks. The final study showcased high performance in cultural creativity and brand design scenarios, demonstrating its cross-domain transfer capability.

# 6 Conclusion

To address the issue of traditional CM technology's heavy reliance on manual experience and the substantial errors in its results, the research proposed an innovative ICM technology grounded in the CNNDL model. The research method utilized the adaptive cuckoo algorithm to select the optimal color parameters from the initial CM samples. It then entered the CNN DL model for convolution operations, batch normalization, and AF calculations. After that, it was combined with the gated RNN model for cyclic operations until the optimal CM result was achieved before being output. The experimental outcomes revealed that the research method improved both efficiency and accuracy. After 20 iterations, the model accuracy of the research approach remained stable at around 93%, and the color harmony score of the resulting CM results was 97.5 points. In practical application testing, when the number of colors in the CM sample increased from 5 to 10, the generation time of the CM results of the research method only increased by 2.2 seconds. In the cultural and creative field, the accuracy and creativity of the CM results of the research method were 90% and 82%, respectively. When the CM sample reached 150, the standard deviation of the CM results generated by the research method stabilized around 1.7. Overall, the method proposed by the research had good CM efficiency and accuracy, which could meet the public's demand for ICM. However, the research experiments focused on controllable laboratory environments and insufficient consideration was given to extreme conditions in complex scenarios. In future studies, the research methods can be further expanded for testing in high-precision application scenarios such as heavy industry and medical health to enhance the comprehensiveness of the research methods.

# References


[1] Shwetha Shetty, Srujana Gali, Denise Augustine, and Srikant N. Sv. Artificial intelligence systems in dental shade-matching: A systematic review. *Journal of Prosthodontics*, 33(6):519–532, 2024.

[2] Ryosuke Sugimura, Toshiki Takamizawa, Ryo Aoki, Ryo Muto, Emika Hirokane, Hayato Kurokawa, et al. Influence of in-office whitening on the color matching and surface characteristics of single-shade resin composites. *Journal of Esthetic and Restorative Dentistry*, 37(2):423–439, 2025.

[3] Kizito Simon, Monica Vicent, Kizito Addah, Deborah Bamutura, Brian Atwiine, Deborah Nanjebe, and Annet Olivia Mukama. Comparison of Deep Learning Techniques in Detection of Sickle Cell Disease. *AIA*, 1(4):252–259, 2023.

[4] Lijun Yao and Li Tang. Evaluation method for colour matching using artificial intelligence technology. *International Journal of Nanotechnology*, 21(6):400–410, 2024.

[5] Chenyang Shen and Mark D. Fairchild. Individual color matching functions from cross-media color-matching experiment. *Color Research & Application*, 50(2):132–143, 2025.

[6] Lu Zhang, Mingwei Li, Yuyang Sun, Xin Liu, Bing Xu, and Li Zhang. Color matching design simulation platform based on collaborative collective intelligence. *CCF Transactions on Pervasive Computing and Interaction*, 4(1):61–75, 2022.

[7] Mingwei Li, Lu Zhang, Yadi Wang, Bei Xing, Xin Liu, Zongyue Tang, et al. Emocolor: An assistant design method for emotional color matching based on semantics and images. *Color Research & Application*, 48(3):312–327, 2023.

[8] Jie Zhou, Tianci Yang, and Wei Zhang. Underwater vision enhancement technologies: A comprehensive review, challenges, and recent trends. *Applied Intelligence*, 53(3):3594–3621, 2023.

[9] Kuankuan Wu, Qiong Fang, Zihao Zhao, and Zhen Li. CoID-LAMP: Color-encoded, intelligent digital LAMP for multiplex nucleic acid quantification. *Analytical Chemistry*, 95(11):5069–5078, 2023.

[10] Amin Haji and Makareem Vadood. Prediction of color coordinates of cotton fabric dyed with binary mixtures of madder and weld natural dyes using artificial intelligence. *Fibers and Polymers*, 24(5):1759–1769, 2023.

[11] Ritika Ghosh and Ashwani Kumar. A hybrid deep learning model by combining convolutional neural network and recurrent neural network to detect forest fire. *Multimedia Tools and Applications*, 81(27):38643–38660, 2022.

[12] Manoutchehr Afshari Nia, Fatemeh Panahi, and Mohammad Ehteram. Convolutional neural network-ANN-E (Tanh): a new deep learning model for predicting rainfall. *Water Resources Management*, 37(4):1785–1810, 2023.

[13] Ebru Pekel Ozmen and Tuba Ozcan. A novel deep learning model based on convolutional neural networks for employee churn prediction. *Journal of Forecasting*, 41(3):539–550, 2022.

[14] Zongren Zhang, Haoran Wu, Haojun Zhao, Yitong Shi, Jiacheng Wang, Hongliang Bai, et al. A novel deep learning model for medical image segmentation with convolutional neural network and transformer. *Interdisciplinary Sciences: Computational Life Sciences*, 15(4):663–677, 2023.

[15] Mehedi Masud, Ahmed Eldin Rashed, and M. Shamim Hossain. Convolutional neural network-based models for diagnosis of breast cancer. *Neural Computing and Applications*, 34(14):11383–11394, 2022.

[16] Haozhong Zhong, Xiao Gao, Bowen Zhao, and Jie Deng. “Matching Rule” for Generation, Modulation and Amplification of Circularly Polarized Luminescence. *Accounts of Chemical Research*, 57(8):1188–1201, 2024.

[17] Saoussen Chaouch, Achraf Moussa, and Neji Ladhari. Textile color formulation methods: A literature review. *Color Research & Application*, 50(1):72–93, 2025.